12. *Tjossem, S. F. Limnol. Oceanogr.* **35,** 1456–1468 (1990).
13. Dawidowicz, P., Pijanowska, J. & Ciechomski, K. *Limnol. Oceanogr.* **35,** 1631–1637 (1990).
14. Ringelberg, J. *J. Plankt. Res.* **13,** 83–89 (1991).
15. Zaret, T. M. *Predation and Freshwater Communities* (University Press of New England, Hanover, New Hampshire, 1980).
16. Lynch, M. & Gabriel, W. *Am. Nat.* **129,** 283–303 (1987).
17. Stearns, S. C. *Bioscience* **39,** 436–445 (1989).
18. Dodson, S. I. *Bioscience* **39,** 447–452 (1989).
19. DuMont, H. J. & De Meester, L. *Rev. Bras. Biol.* **50,** 867–874 (1990).
20. Andrusak, H. & Northcote, T. G. *J. Fish. Res. Bd. Can.* **28,** 1259–1268 (1971).
21. Peacock, A. H. *Can. J. Zool.* **60,** 1446–1462 (1982).
22. Alcock, J. *Animal Behavior* (Sinauer, Sunderland, 1975).
23. Northcote, T. G. & Clarotto, R. *Verh. Int. Verein. Limnol.* **19,** 2378–2393 (1975).
24. Neill, W. E. *Oecologia* **61,** 175–181 (1984).

ACKNOWLEDGEMENTS. I thank T. Shardlow, R. Newsome, K. Ashley, A. Redenback, J. Barrett-Lennard, D. Robinson and D. Dolecki for assistance, the Center for Limnology, University of Wisconsin, Madison for facilities and S. Carpenter, B. DeStasio, T. Frost, L. Rudstam, D. Schindler and W. Wurtsbaugh for comments. Research was supported in part by the Natural Science and Engineering Research Council of Canada, the British Columbia Ministry of Labour, and the University of British Columbia.

A chloride channel widely expressed in epithelial and non-epithelial cells

Astrid Thiemann, Stefan Gründer, Michael Pusch & Thomas J. Jentsch*

Centre for Molecular Neurobiology (ZMNH), Hamburg University, Martinistrasse 52, D-2000 Hamburg 20, Germany

CHLORIDE channels have several functions, including the regulation of cell volume[1,2], stabilizing membrane potential[3,4], signal transduction[5,6] and transepithelial transport[7]. The plasma membrane Cl^- channels already cloned belong to different structural classes: ligand-gated channels[5,6], voltage-gated channels[8,9], and possibly transporters of the ATP-binding-cassette type (if the cystic fibrosis transmembrane regulator[10] is a Cl^- channel[11–13]). The importance of chloride channels is illustrated by the phenotypes that can result from their malfunction: cystic fibrosis, in which transepithelial transport is impaired, and myotonia[3], in which ClC-1, the principal skeletal muscle Cl^- channel, is defective[9]. Here we report the properties of ClC-2, a new member of the voltage-gated Cl^- channel family. Its sequence is ~50% identical to either the *Torpedo* electroplax Cl^- channel, ClC-0 (ref. 8), or the rat muscle Cl^- channel, ClC-1 (ref. 9). Isolated initially from rat heart and brain, it is also expressed in pancreas, lung and liver, for example, and in pure cell lines of fibroblastic, neuronal, and epithelial origin, including tissues and cells affected by cystic fibrosis. Expression in *Xenopus* oocytes induces Cl^- currents that activate slowly upon hyperpolarization and display a linear instantaneous current–voltage relationship. The conductivity sequence is $Cl^- \geq Br^- > I^-$. The presence of ClC-2 in such different cell types contrasts with the highly specialized expression of ClC-1 (ref. 9) and also with the cloned cation channels, and suggests that its function is important for most cells.

A complementary DNA encoding the rat skeletal muscle Cl^- channel ClC-1 (ref. 9) was used to screen cDNA libraries from rat heart and brain under relaxed stringency. Sequencing of positive clones indicated the presence of novel Cl^- channel (ClC-2) messenger RNAs that were identical in both tissues. Clones were more abundant in the brain library, from which several large (>3 kilobases (kb)) clones were isolated, the largest of which was fully sequenced (Fig. 2). The putative initiator methionine is followed by a hydrophobic stretch of ~11 amino acids, a feature not found in other channels[8,9] of this family. The sequence predicts a 907-amino-acid protein of relative molecular mass ~99,000 having a transmembrane topology similar to that of related Cl^- channels[8,9]. Overall homology to the *Torpedo* channel ClC-0 is 49%, and 55% to the rat muscle Cl^- channel ClC-1. Divergence is greatest at the N- and C-termini and between domains D12 and D13.

Northern analysis revealed that ClC-2 is expressed in all the tissues that we examined (Fig. 1*a*). In addition to a common mRNA of ~3.3 kb, larger species (~4.5 kb) were detected in some tissues (for example, kidney and brain) and may represent splice or polyadenylation variants. Established cell lines were used to investigate expression in defined cell types (Fig. 1*b*). The ~3.3-kb transcript was found in all these cell lines, with the additional ~4.5-kb band being detected primarily in human and monkey cells. ClC-2 is thus transcribed in typical fibroblast (3T3) and epithelial cells (T84; a human colon cell line[14], CFPAC-1; a human pancreatic cystic fibrosis cell line[15], and LLC-PK_1), as well as in neuronal-like cells (Neuro-2a, PC-12). In some tissues and cells (for example, heart and skeletal muscle, A10) ClC-2 is co-expressed with ClC-1 (ref. 9). It will be interesting to see if these homologous proteins form hetero-oligomeric channels with new properties.

In *Xenopus* oocytes, Cl^- currents could not be expressed from

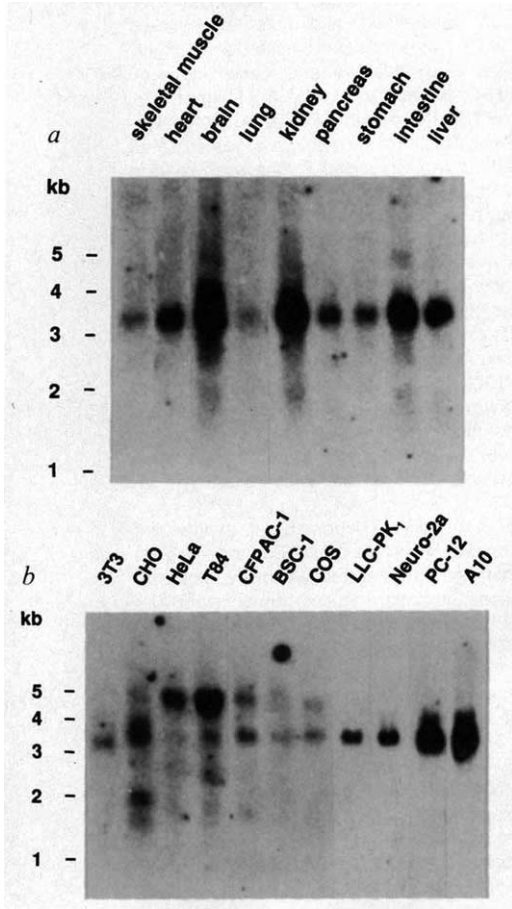

FIG. 1 Northern analysis of ClC-2 expression. *a*, Expression in different rat tissues; *b*, expression in established cell lines.
METHODS. RNA was extracted from several tissues and cell lines and enriched for poly(A)$^+$ tracts: 10 μg each (by absorbance at 260 nm) (15 μg for Neuro-2a and LLC-PK_1) were run on agarose gels containing formaldehyde. Equal loading and absence of degradation was additionally checked by staining with ethidium bromide. The size standard is a ^{32}P-labelled 1-kb DNA ladder (BRL). After transfer to nylon membranes, blots were hybridized under high stringency with clone λb12-2 labelled with ^{32}P, and autoradiographed. Cell lines are: 3T3, NIH3T3 mouse fibroblasts; A10, rat aorta smooth muscle (CRL1476); BSC-1, African green monkey kidney (CCL26); CFPAC-1, human pancreatic tumour expressing the CF phenotype[15]; CHO, CHO-K1 Chinese hamster ovary cells (CCL61); COS, COS-7 SV40 transformed monkey kidney (CRL1651); HeLa, human epitheloid cervix carcinoma (CCL2); LLC-PK_1, pig kidney (CL101); Neuro-2a, mouse neuroblastoma (CCL131); PC-12, rat adrenal pheochromocytoma (CRL1721); T84, human colon carcinoma (CCL248). Culture conditions were as recommended for each specific line.

* To whom correspondence should be addressed.

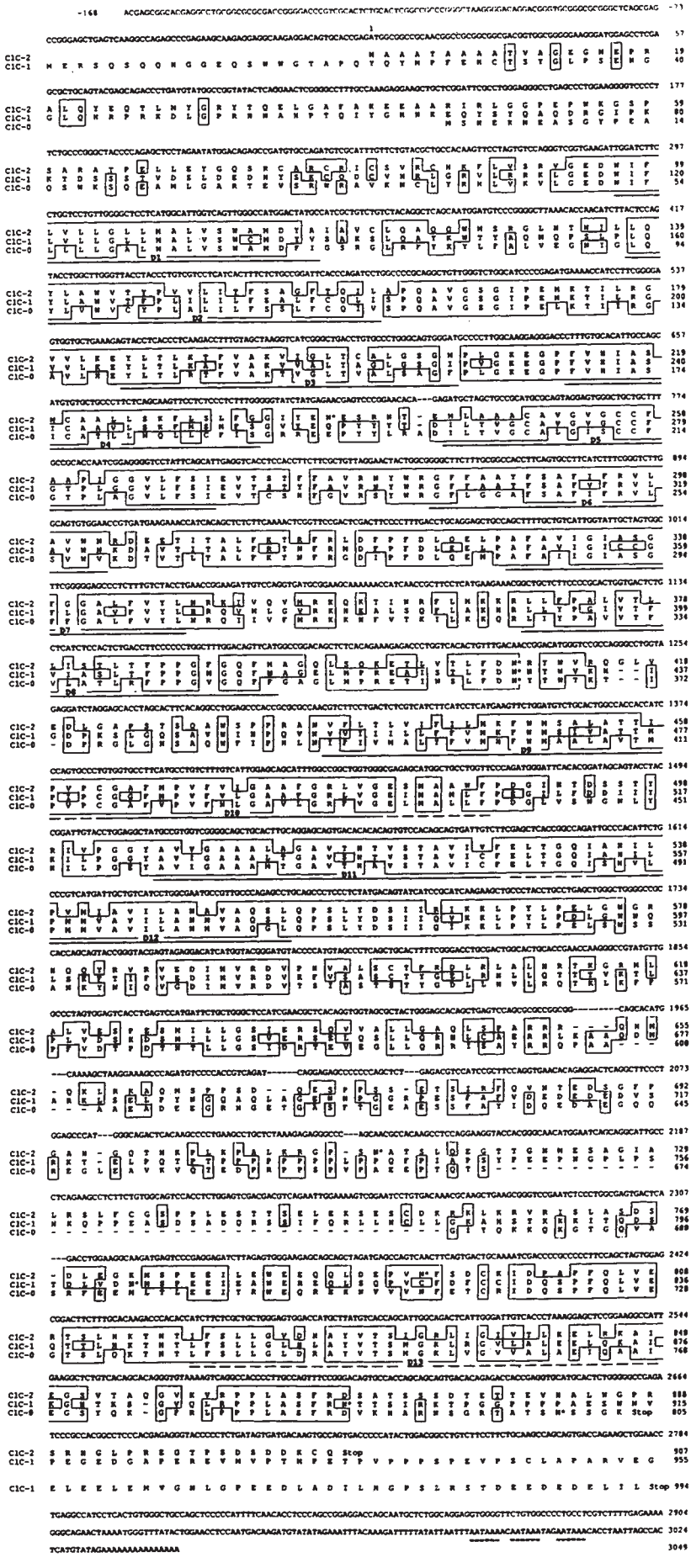

FIG. 2 Primary structure of chloride channel ClC-2. Nucleotide sequence of ClC-2 and alignment of its deduced amino-acid sequence with that of the rat skeletal muscle Cl^- channel ClC-1 (ref. 9) and the *Torpedo* channel ClC-0 (ref. 8). Conserved residues are boxed, putative transmembrane domains[30] underlined, and potential *N*-linked glycosylation sites indicated by asterisks. A highly conserved glycosylation site is present between D8 and D9, and additional ones at positions 238, 712 and 794. Polyadenylation signals are double-underlined. The initiator methionine was assigned to the first ATG preceding a long open reading frame. This ATG, as well as a second one following 45 base pairs (bp) downstream in frame, is surrounded by sequence fulfilling the requirements for eukaryotic initiation[31]. As there is no upstream stop codon in frame, we cannot be absolutely sure whether this represents the authentic initiator ATG. But we cannot miss much upstream sequence (length of cDNA, excluding the poly(A) tail, is 3,202 bp, versus a message size of ~3.3 kb by northern analysis (Fig. 1)), and one independent clone terminated within 5 bp, and 2 clones within 150 bp of the shown 5′ end. Moreover, functional Cl^- channels could be expressed starting from this ATG (Fig. 3).

METHODS. An oligo(dT) primed rat brain cDNA library in λZAPII (a gift from S. Morley and W. Meyerhof) and a rat heart cDNA library (Clontech) were screened under reduced stringency (in 5× SSC, 5×Denhardt's solution, 25% formamide, 0.1% SDS at 42 °C) with a radiolabelled ClC-1 (ref. 9) cDNA probe (extending from bp 990 to 1,881). Positive clones were confirmed by sequencing and used to rescreen the brain library at high stringency. The sequence shown derives from clone λb12-2 (except for the poly(A) tail, which derives from clone λb9), which was fully sequenced on both strands using T7 DNA polymerase in the chain termination method. The sequence has been deposited in the EMBL/GenBank database under accession number X64139.

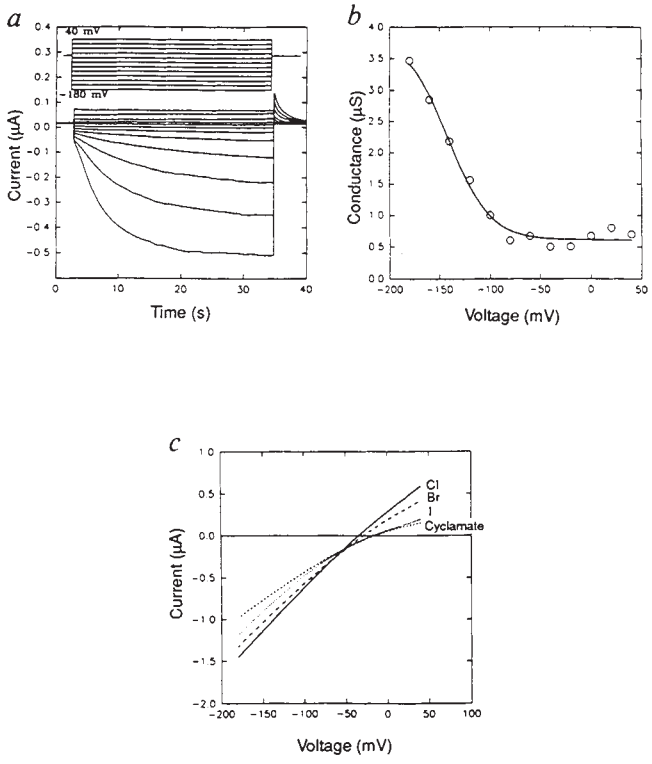

FIG. 3 Electrophysiological analysis of ClC-2 expressed in *Xenopus* oocytes. *a*, Voltage-clamp traces. Voltage was clamped for 32 s from a holding potential of −30 mV to values between −180 and +40 mV in 20 mV steps (inset), and the current necessary to clamp the oocyte was recorded. Note that currents activate slowly upon hyperpolarization, and that deactivation is much faster. *b*, Quasi-steady-state conductance as a function of voltage (measured after clamping for 32 s to the indicated potential); reversal potential was assumed to be −30 mV. The curve fitted is of the form $G(V)=G_0+G_1/(1+\exp((V-V_0)/K))$. Note that conductance between +40 and −80 mV is constant and similar to that of control oocytes, suggesting that the vast majority of ClC-2 channels is not open. Conductance increases steeply at voltages more negative than −100 mV without saturating at −180 mV. Mean conductance at −180 mV (after at least 30 s) was 8.2 ± 0.8 (s.e.m., $n=12$) μS for cRNA-injected oocytes, and 2.2 ± 0.5 (s.e.m., $n=9$) μS for non-injected controls. In the range between 0 and 20 mV, conductance averaged to 1.4 ± 0.2 (s.e.m., $n=12$) μS for injected, and 2.9 ± 0.9 (s.e.m., $n=9$) μS for control oocytes. *c*, Instantaneous current-voltage (I-V) relationships of activated channels in the presence of different extracellular anions (from a different oocyte). Immediately after activation by hyperpolarization (−180 mV for 32 s), fast voltage ramps (0.5 s) in positive or negative directions were used to minimize effects of deactivation. Results were not significantly different from those obtained by tail-current analysis. Ion selectivity was tested by partially replacing 80 mM extracellular chloride with iodide, bromide, or cyclamate. Data were not corrected for liquid junction potentials. The reversal potential ($I=0$) shifts towards positive voltages on chloride removal, indicating a chloride-selective channel. Note that the I-V curve for Cl^- is nearly linear, and that the channel displays a $Cl^- \geq Br^- > I^-$ selectivity sequence.

METHODS. Recombinant polymerase chain reaction (PCR)[32] was used to construct plasmid ptm1-b12-2 in which 83 bp of 5′ sequence immediately preceding the initiator ATG of ClC-0 (ref. 8) was placed in front of the first ATG of ClC-2 clone λb12-2. The resulting chimaeric PCR product was digested with *Xho*I and ligated at the 54-bp *Xho*I site to clone λb12-2. The sequence of the new fragment was fully verified. This does not introduce any new amino acids into the resulting protein. After linearization of the construct, capped RNA was synthesized *in vitro* using T7 RNA polymerase, about 50 ng of which was injected into *Xenopus* oocytes prepared and handled as described[33]. They were stored and analysed in ND96 solution (96 mM NaCl, 2 mM KCl, 1.8 mM $CaCl_2$, 1 mM $MgCl_2$, 5 mM HEPES, pH 7.6), or in ND96, in which 80 mM NaCl was replaced by 80 mM NaI, NaBr, or sodium cyclamate. Electrophysiological analysis was at room temperature 2–4 days after injection using standard 2-electrode-voltage clamp technique and pCLAMP software.

the intact, putative full-length cDNA. We replaced sequence 5′ to the first ATG by 5′ non-translated sequence from ClC-0, a previously successful strategy[9]. Expression of derived cRNA in *Xenopus* oocytes led to Cl^- currents that were not detectable under resting conditions, but increased slowly (within tens of seconds) after hyperpolarization. An activation by hyperpolarization is also found with ClC-0 (refs 8, 16, 17), but not with ClC-1 (ref. 9). With ClC-2, activation began at about −90 mV and did not saturate even at −180 mV (Fig. 3*a*, *b*). Stepping back to the holding potential (−30 mV) caused deactivation within seconds. Instantaneous I-V curves of activated channels revealed a linear current-voltage relationship (Fig. 3*c*). Partial replacement of extracellular chloride is indicative of an anion-selective channel with a $Cl^- \geq Br^- > I^-$ conductivity sequence. Although iodide blocks ClC-0 (refs 16, 17), it permeates ClC-2. Extracellular 9-anthracene carboxylic acid (1 mM) and diphenylaminecarboxylate (1 mM), which are Cl^- channel inhibitors but also have other effects[18], partially (~50%) inhibited the conductance, whereas 1 mM DIDS (4,4′-diisothiocyano-2,2′-disulphonic acid) was almost ineffective (data not shown).

As ClC-2 is broadly expressed in different tissues and in cells of such varied origin as epithelial, fibroblast and neuronal cells, it may share some important housekeeping role in these cells. The channel is closed at physiological voltages, so perhaps some other mechanism of activation (in addition to hyperpolarization) exists *in vivo*. The expression of ClC-2 in T84 epithelial cells is especially interesting and was verified by cloning partial T84 ClC-2 cDNAs (unpublished results). T84 cells have served as a model system for Cl^- transport, highly relevant for cystic fibrosis (CF). They express at least four different Cl^- channels, three of which conduct iodide better than chloride and are outward-rectifying (volume-sensitive[1,19] and Ca^{2+}-activated[20–22] channels, and an obscure[20,23] 40–60-pS channel, formerly thought to be affected in CF (for review, see ref. 7)). The fourth channel has a time-independent linear I-V relationship, a Cl > I selectivity, and probably mediates the cyclic AMP-activated current defective in CF (refs 20, 21, 24). On the basis of the instantaneous I-V relationhsip, selectivity and pharmacology, ClC-2 most closely resembles this latter channel. It is unclear, however, whether the channel affected in CF can be activated by strong hyperpolarization, and whether ClC-2 can somehow interact with the cystic fibrosis transmembrane regulator (CFTR)[10], the CF gene product.

CFTR, previously thought to regulate Cl^- channels[25], is now believed to be a cAMP-activated channel itself. This is based on two main findings: first, CFTR expression in different cells (for example, CFPAC-1 (ref. 26), 3T3 (ref. 11), HeLa (refs 11, 27), CHO (refs 11, 28), T84 (ref. 11), Sf9 (ref. 12)) induces cAMP-activated Cl^- currents. It was unlikely that all these cells would have pre-existent similar Cl^- channels serving as targets for CFTR. Our work nearly invalidates this argument, though we did not test non-mammalian cells because of expected difficulties in cross-species hybridization. Second, and most convincing, mutagenesis of CFTR changes ion selectivity[13] and cAMP-dependence[27,29] of currents. Thus, certain similarities of ClC-2 with the Cl^- channel affected in CF are tantalizing, but probably coincidence. The functions of ClC-2 remain to be identified, but these are important because it is expressed in cells affected by CF. □

Received 6 November; accepted 10 December 1991.

1. Worrel, R. T., Butt, A. G., Cliff, W. H. & Frizzell, R. A. *Am. J. Physiol.* **256,** C1111-C1119 (1989).
2. Strange, K. *Am. J. Physiol.* **260,** F225-F234 (1991).
3. Steinmeyer, K. *et al. Nature* **354,** 304-308 (1991).
4. Bretag, A. H. *Physiol. Rev.* **51,** 618-724 (1987).
5. Grenningloh, G. *et al. Nature* **328,** 215-220 (1987).
6. Schofield, P. R. *et al. Nature* **328,** 221-227 (1987).
7. Welsh, M. J. *FASEB J.* **4,** 2718-2725 (1990).
8. Jentsch, T. J., Steinmeyer, K. & Schwarz, G. *Nature* **348,** 510-514 (1990).
9. Steinmeyer, K., Ortland, C. & Jentsch, T. J. *Nature* **354,** 301-304 (1991).
10. Riordan, J. R. *et al. Science* **245,** 1066-1073 (1989).

11. Anderson, M. P. *et al. Science* **251,** 679–682 (1991).
12. Kartner, N. *et al. Cell* **64,** 681–691 (1991).
13. Anderson, M. P. *et al. Science* **253,** 202–205 (1991).
14. Dharmsathaphorn, K., McRoberts, J. A., Mandel, K. G., Tisdale, L. D. & Masui, H. *Am. J. Physiol.* **246,** G204–G208 (1984).
15. Schoumacher, R. A. *et. al. Proc. natn. Acad. Sci. U.S.A.* **87,** 4012–4016 (1990).
16. Bauer, C. K., Steinmeyer, K., Schwarz, J. R. & Jentsch, T. J. *Proc. natn. Acad. Sci. U.S.A.* **88,** 11052–11056 (1991).
17. Miller, C. & Richard, E. A. in *Chloride Channels and Carriers in Nerve, Muscle, and Glial Cells* (eds Alvarez-Leefsmans, F. J. & Russel, J. M.) 383–405 (Plenum, New York 1990).
18. Kreusel, K.-M., Fromm, M., Schulzke, J.-D. & Hegel, U. *Am. J. Physiol.* **261,** C574–C582 (1991).
19. Solc, C. K. & Wine, J. J. *Am. J. Physiol.* **261,** C658–C674 (1991).
20. Cliff, W. H. & Frizzell, R. A. *Proc. natn. Acad. Sci. U.S.A.* **87,** 4956–4960 (1990).
21. Anderson, M. P. & Welsh, M. J. *Proc. natn. Acad. Sci. U.S.A.* **88,** 6003–6007 (1991).
22. Worrell, R. T. & Frizzell, R. A. *Am. J. Physiol.* **260,** C877–C882 (1991).
23. Ward, C. L., Krouse, M. E., Gruenert, D. C., Kopito, R. R. & Wine, J. J. *Proc. natn. Acad. Sci. U.S.A.* **88,** 5277–5281 (1991).
24. Tabcharani, J. A., Low, W., Elie, D. & Hanrahan, J. W. *FEBS Lett.* **270,** 157–164 (1990).
25. Hyde, S. C. *et al. Nature* **346,** 362–365 (1990).
26. Drumm, M. L. *et al. Cell* **62,** 1227–1233 (1990).
27. Rich, D. P. *et al. Science* **253,** 205–207 (1991).
28. Tabcharani, J. A., Chang, X.-B., Riordan, J. R. & Hanrahan, J. W. *Nature* **352,** 628–631 (1991).
29. Cheng, S. H. *et al. Cell* **66,** 1027–1036 (1991).
30. Kyte, J. & Doolittle, R. F. *J. molec. Biol.* **157,** 105–132 (1982).
31. Kozak, M. *J. Cell Biol.* **115,** 887–903 (1991).
32. Higuchi, R. in *PCR Technology* (ed. Erlich, H. A.) 61–70 (Stockton, New York, 1989).
33. Colman, A. in *Transcription and Translation* (eds Hames, B. D. & Higgins, S. J.) 271–302 (IRL, Oxford, 1984).

ACKNOWLEDGEMENTS. We thank B. König for technical assistance, K. Steinmeyer for help with northern blots and for discussion, and S. Morley and W. Meyerhof for the rat brain cDNA library. This work was supported, in part, by the BMFT, the US Cystic Fibrosis Foundation, and the Deutsche Forschungsgemeinschaft.

Delay in vesicle fusion revealed by electrochemical monitoring of single secretory events in adrenal chromaffin cells

Robert H. Chow, Ludolf von Rüden & Erwin Neher*

Max-Planck-Institut für biophysikalische Chemie, Postfach 2841, Am Fassberg, D-3400 Göttingen, Germany

IN synapses, a rise in presynaptic intracellular calcium leads to secretory vesicle fusion in less than a millisecond, as indicated by the short delay from excitation to postsynaptic signal[1–4]. In non-synaptic secretory cells, studies at high time resolution have been limited by the lack of a detector as fast and sensitive as the postsynaptic membrane. Electrochemical methods may be sensitive enough to detect catecholamines released from single vesicles[5,6]. Here, we show that under voltage-clamp conditions, stochastically occurring signals can be recorded from adrenal chromaffin cells using a carbon-fibre electrode as an electrochemical detector. These signals obey statistics characteristic for quantal release; however, in contrast to neuronal transmitter release, secretion occurs with a significant delay after short step depolarizations. Furthermore, we identify a pedestal or 'foot' at the onset of unitary events which may represent the slow leak of catecholamine molecules out of a narrow 'fusion pore' before the pore dilates for complete exocytosis.

Isolated bovine chromaffin cells were used to study catecholamine release under patch-clamp whole-cell recording conditions. We applied short step depolarizations to open voltage-gated calcium channels[7], thereby injecting calcium to activate secretion[8]. When the tip of a carbon-fibre electrode[5,9,10] was placed less than 1 μm from the cell to record in amperometric mode, spike-like current transients were seen at variable times after the onset of depolarizing pulses (see Fig. 1*a*). These signals occurred rarely or not at all, unless the cell had been stimulated; on stimulation they appeared with a frequency that peaked shortly after the voltage step and that subsequently decayed over about 100 ms. Furthermore, they were seen only if the potential applied to the carbon-fibre electrode was greater than about 250 mV (exceeding the oxidation potential for catecholamines). When the detector was moved several microns away from the cell, the signals became smaller and slower. Stimulating with longer depolarizations generally led to an increase in the number and frequency of unitary events, not to an increase in their individual size (Fig. 1*b*). These observations suggest that the signals represent packages of oxidizable substance being secreted from the cell, in agreement with a previous report on unclamped cells[5].

TABLE 1 Single secretory events follow a Poisson distribution

Cells	n_0	n_1	n_2	n_3	$n_{>3}$	N	events
A							
Observed	45	52	26	7	3	133	139
Calc. ($m=1.01$)	47	49	26	9	2		
B							
Observed	8	18	17	12	10	65	133
Calc. ($m=2.05$)	8	17	18	12	10		
C							
Observed	15	28	20	8	3	74	105
Calc. ($m=1.42$)	18	25	18	9	4		
D							
Observed	28	19	11	0	0	58	41
Calc. ($m=0.71$)	29	20	7	2	0		

Three cells with a low probability of release were selected for analysis. Cells A, B, C and D were repetitively stimulated every 5 s by depolarizing pulses to +10 mV for 25 ms (A, C) or 50 ms (B, D). D was, in fact, the same cell as C, but at a much later time in the experiment, when the release probability had decreased. Each discernible current transient, regardless of size, was counted as one event. $n_{0,1,2,3,\ldots,x}$: numbers of times that pulses elicited 0, 1, 2, 3 . . . , x events during the 5-s interval after a pulse. Calculated numbers: from Poisson's law

$$P_x = n_x/N = e^{-m}m^x/x!.$$

N, Total number of step depolarizations.
m, (total number of events)$/N = (n_1 + 2n_2 + 3n_3 + \cdots xn_x)/N$.

Another way to monitor secretion from single cells is to record the membrane capacitance[8,11]. This electrical parameter is proportional to cell surface area and increases when vesicles fuse with the plasma membrane during exocytosis. When a cell was stimulated repetitively (Fig. 2), the time-averaged signal of the carbon-fibre electrode closely resembled the derivative of the capacitance trace, thus confirming that both quantities reflect rate of transmitter release. In another cell (data not shown), short depolarizing pulses each elicited an average of 1.05 unitary events and a 13-fF increment in capacitance. Assuming that each event is due to a single vesicle and that each vesicle contributes 2.5 fF (as suggested from previous measurements[8] and from morphometry), we conclude that the carbon-fibre electrode detected about 15–25% of the quanta released. This compares well with the fraction of the cell surface area in closest apposition to the detector surface (see Fig. 1 legend).

Amperometric currents from secreting chromaffin cells arise almost exclusively from oxidation of catecholamine molecules[6], and each molecule contributes two electronic charges[12]. Thus, one can estimate the number of catecholamine molecules per transient from the total charge of the unitary signal. Figure 1*c* shows a histogram of the integrals of the current transients from three cells. From its mean the number of molecules detected can be calculated as 2.4–3.2 million (see Fig. 1 legend), agreeing with previous estimates (3×10^6 molecules) for single bovine chromaffin granules[13].

For synapses the number of vesicles released per stimulus follows binomial or Poisson statistics[1]. As shown in Table 1, such statistics also apply to secretion from chromaffin cells. Although the unitary events are not as uniform as miniature synaptic currents, they are generally well separated in time (for submaximal stimuli), making it possible to count them directly (something not possible for postsynaptic signals except at very low temperatures and low calcium[14]).

* To whom correspondence should be addressed.